Improvement in coercivity, thermal stability, and corrosion resistance of sintered Nd–Fe–B magnets with $Dy_{80}Ga_{20}$ intergranular addition*

Beibei Zhou(周贝贝)[1], Xiangbin Li(李向斌)[1], Xuejing Cao(曹学静)[1], Gaolin Yan(严高林)[1,†], and Aru Yan(闫阿儒)[2]

[1] School of Physics and Technology, Wuhan university, Wuhan 430072, China
[2] Zhejiang Province Key Laboratory of Magnetic Materials and Application Technology, Key Laboratory of Magnetic Materials and Devices, Ningbo Institute of Materials Technology and Engineering, Chinese Academy of Sciences, Ningbo 315201, China

(Received 19 May 2016; revised manuscript received 9 August 2016; published online 30 September 2016)

To investigate the coercivity, corrosion resistance, and thermal stability of Nd–Fe–B magnets, their properties were investigated at room and high temperature before and after doping with $Dy_{80}Ga_{20}$ (at.%) powder. The coercivity of the magnets increased from the undoped value of 12.72 kOe to a doped value of 21.44 kOe. A micro-structural analysis indicates that a well-developed core-shell structure forms in the magnets doped with $Dy_{80}Ga_{20}$ powder. The improvement in magnetic properties is believed to be related to the refined and uniform matrix grains, continuous grain boundaries, and a hardened $(Nd, Dy)_2Fe_{14}B$ shell surrounding the matrix grains. Additionally, the doped magnets exhibit an obvious improvement in thermal stability. For the magnets with added $Dy_{80}Ga_{20}$ powder, the temperature coefficients of remanence (α) and coercivity (β) increased to $-0.106\%\ ^{\circ}C^{-1}$ and $-0.60\%\ ^{\circ}C^{-1}$ over the range 20–100 °C, compared to temperature coefficients of $-0.117\%\ ^{\circ}C^{-1}$ (α) and $-0.74\%\ ^{\circ}C^{-1}$ (β) in the regular magnets without $Dy_{80}Ga_{20}$ powder. The irreversible loss of magnetic flux (Hirr) was investigated at different temperatures. After being exposed to 150 °C for 2 h, the Hirr of magnets with 4 wt.% $Dy_{80}Ga_{20}$ decreased by ∼95% compared to that of the undoped magnets. The enhanced temperature coefficients and Hirr indicate improved thermal stability in the doped Nd–Fe–B magnets. The intergranular addition of $Dy_{80}Ga_{20}$ also improved the corrosion resistance of the magnets because of the enhanced intergranular phase. In a corrosive atmosphere for 96 h, the mass loss of the sintered magnets with 4 wt.% $Dy_{80}Ga_{20}$ was 2.68 mg/cm^2, less than 10% of that suffered by the undoped magnets (28.1 mg/cm^2).

Keywords: Nd–Fe–B permanent magnet, magnetic property, thermal stability, corrosion resistance

PACS: 75.50.Ww, 75.30.–m, 65.40.–b, 82.45.Bb **DOI:** 10.1088/1674-1056/25/11/117504

1. Introduction

Since their discovery in 1984, Nd–Fe–B sintered magnets have been widely applied in products such as sensors, motors, and generators because of their excellent magnetic properties.[1,2] In particular, Nd–Fe–B sintered magnets are frequently applied in high-temperature environments such as hybrid electric vehicles.[3] However, the magnetic performance of Nd–Fe–B sintered magnets declines sharply at temperatures above 100 °C, which greatly limits their application. Therefore, it is desirable to enhance the magnetic properties and thermal stability of Nd–Fe–B magnets at high working temperatures.

Composed of an $Nd_2Fe_{14}B$ matrix phase and intergranular Nd-rich phases, Nd–Fe–B magnets exhibit high magnetic performance in the matrix phase because of their excellent intrinsic magnetic anisotropy field. Furthermore, the intergranular phase around the matrix phase improves the magnetic properties by reducing the exchange coupling between neighboring ferromagnetic grains.[4–6] However, with the lower electrode potential of the Nd, Nd–Fe–B magnets suffer from corrosion in the Nd-rich intergranular phase. To improve the corrosion resistance of these magnets, the composition of the Nd-rich phase can be modified.

As the intrinsic anisotropy field of $Dy_2Fe_{14}B$ is 15.8 T, which is about twice the value of 7.5 T for $Nd_2Fe_{14}B$, the coercivity of Nd–Fe–B magnets can be effectively improved by the addition of Dy.[7,8] In recent years, Nd–Fe–B sintered magnets with the intergranular addition of Dy have been widely investigated. It can be inferred from these studies that intergranular Dy addition enhances the magnetic properties of Nd–Fe–B sintered magnets more effectively than the conventional method of Dy element addition, with less decline in the remanence.[9–14] Recent research by Zhang *et al.*[15] has indicated that the thermal stability of Nd–Fe–B sintered magnets can be improved by Dy addition, and it is known that doping with Cu, Al, Ga, and Nb provides a slight enhancement in the coercivity of Nd–Fe–B magnets.[16–22] Furthermore, the addition of Cu, Al, and Ga may also improve the corrosion resistance of doped magnets because of their relatively higher electrode potential.[21]

According to the Dy–Ga binary phase diagram, a compo-

*Project supported by the Ministry of Science and Technology of China (Grant Nos. 2014DFB50130 and 2011CB612304) and the National Natural Science Foundation of China (Grant Nos. 51172168 and 51072139).

†Corresponding author. E-mail: gaolinyan@whu.edu.cn

© 2016 Chinese Physical Society and IOP Publishing Ltd

sition with a low melting point was selected for this study. A $Dy_{80}Ga_{20}$ alloy powder was introduced into the Nd–Fe–B sintered magnets by intergranular addition. Under heat treatment of Nd–Fe–B magnets, the doped $Dy_{80}Ga_{20}$ powder modified the Nd-rich intergranular phase in the magnets, giving a highly magnetic $(Dy, Nd)_2Fe_{14}B$ shell on the surface of the matrix phase. Thus, the coercivity of the doped Nd–Fe–B magnets was evidently improved. The enhancement of thermal stability and corrosion resistance in the doped magnets was also investigated in this study.

2. Experimental procedure

An alloy with a nominal composition of $(Pr_{80}Nd_{20})_{31}Fe_{bal}B$ (wt.%) was prepared by strip casting. Specifically, the obtained flakes were first broken into smaller and more frangible pieces by hydrogen decrepitation, and the smaller flakes were then impacted into powder by nitrogen in the jet-milling process (OLM-100T). A Laser Particle Size Analyzer (HELOS/RODOS/M) determined the average particle diameter of the obtained powder to be ~ 2.2 μm.

The $Dy_{80}Ga_{20}$ (at.%) alloy ingots were obtained through induction melting in a high-purity argon atmosphere. The ingots were crushed into small pieces mechanically, and then the pieces were milled into powder through high-energy ball milling for 60 min, with gasoline used as the protection medium. After milling, the mean particle size of the $Dy_{80}Ga_{20}$ powder was ~ 2.5 μm.

The fine $Dy_{80}Ga_{20}$ powder was uniformly mixed with the master powder in a three-dimensional mixer for 5 h. The mixed powder was compacted under a magnetic field of 1800 kA/m and further pressed by a cold isostatic press (LDJ200/600-300) at 200 MPa. The green compacts were sintered at 1010 °C for 2 h with vacuum protection, followed by annealing heat treatment at 800 °C and 520 °C for 2 h each.

The magnetic properties of the sintered magnets at room and relatively high temperatures were measured by a Permanent Magnet Material High Temperature Measurement Device (NIM-500C). Moreover, the temperature coefficients of remanence (α) and coercivity (β) were calculated based on the magnetic properties at different temperatures. The microstructure and elemental distribution were observed under an Electron Probe Micro-Analyzer (JXA-8230) with a Wavelength Dispersive Spectrometer (WDS). The phase transition temperature of the $Dy_{80}Ga_{20}$ powder was tested by Differential Scanning Calorimetry (DSC) at a heating rate of 10 °C/min. The DSC curve indicated that the fusion point of $Dy_{80}Ga_{20}$ alloy was about 945 °C, which is below the corresponding temperature for sintered Nd–Fe–B. The irreversible loss of magnetic flux was detected by a Helmholtz Coil after being exposed at relatively high temperatures (60–150 °C) for 2 h. The density of the Nd–Fe–B sintered magnets was investigated based on the Archimedes principle.

In the accelerated corrosion test, the prepared cylindrical samples ($\pi \cdot 5^2$ mm$^2 \times 5$ mm), which had been polished by 1000# sandpaper, were placed in a 120 °C, 2 bar, and 100% relative humidity atmosphere for 24, 48, 72, and 96 h, respectively. The tested samples were then subjected to Ultrasonic Vibration for 10 min to remove the corrosion products on the surface. The sintered magnets with 0–4 wt.% $Dy_{80}Ga_{20}$ were weighed by a microbalance before and after the corrosion tests. The weight differential was then calculated to characterize the corrosion weight loss of the magnets according to the surface area.

3. Results and discussion

SEM images of the starting magnet and the doped ones are shown in Figs. 1(a)–1(c), where the dark gray and white regions correspond to the matrix phase and the intergranular phase, respectively. As shown in Fig. 1(a), the intergranular phase of the starting magnets was mainly rounded or rectangular, and there was little continuous grain boundary layer between the two ferromagnetic matrix phases. This indicates that the matrix phase was not isolated well enough for the

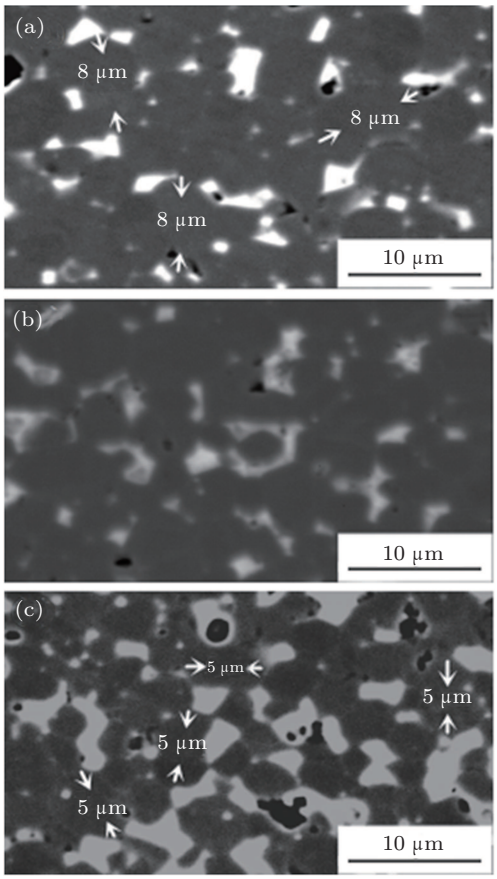


Fig. 1. EPMA back-scattered images of (a) the starting magnet, (b) the magnet with 2 wt.% $Dy_{80}Ga_{20}$, and (c) the magnet with 4 wt.% $Dy_{80}Ga_{20}$.

poor wettability between the intergranular phase and the matrix phase. The 2 wt.% $Dy_{80}Ga_{20}$ magnet in Fig. 1(b) exhibits an improved intergranular phase of a thin strip, which effectively isolates the matrix grain and demagnetizes the exchange coupling.[21] The size of the matrix phase was optimized by the addition of $Dy_{80}Ga_{20}$ powder. The grain size of the starting magnets is ~3–8 μm in Fig. 1(a). However, the addition of up to 4 wt.% $Dy_{80}Ga_{20}$ powder results in a more uniform and smaller grain size of ~3–5 μm, as shown in Fig. 1(c).

The magnetic properties of the Nd–Fe–B sintered magnets are listed in Table 1. Because of the relatively lower intrinsic anisotropy field of the $Nd_2Fe_{14}B$, the coercivity of the starting magnets was just 12.72 kOe, although the energy product and remanence of these magnets were up to 46.63 MGOe and 13.82 kGs, respectively.[1,2] As the intrinsic anisotropy field of $Dy_2Fe_{14}B$ is 15.8 T, which is over twice the 7.5 T of $Nd_2Fe_{14}B$, the coercivity of the magnets with added $Dy_{80}Ga_{20}$ was effectively improved.[4] With 1 wt.% $Dy_{80}Ga_{20}$, the coercivity increased to 16.41 kOe, whereas the remanence decreased to 13.31 kGs. This indicates that the coercivity of the magnets increased by ~29%, but the corresponding decrease in remanence was only ~3.7%. The enhancement of the doped magnets can be attributed to the diffusion of Dy into the matrix phase, which constitutes the highly magnetic $(Dy, Nd)_2Fe_{14}B$ phase. The decline in Br is likely to be related to the nucleation of the magnetization reversal domain with the addition of Dy. As the distribution of Dy is concentrated on the surface of the matrix grain, there is only a minor reduction in remanence. As more $Dy_{80}Ga_{20}$ alloy powder is added to the Nd–Fe–B magnets, the coercivity continues to increase. When the content of $Dy_{80}Ga_{20}$ powder reached 4 wt.%, the coercivity of the doped magnets reached 21.44 kOe, an increase of 68% over the undoped magnets. At the same time, the remanence of the doped magnets decreased to 12.28 kGs, ~11% lower than that of the starting magnets. In the Nd–Fe–B magnets with 4 wt.% $Dy_{80}Ga_{20}$, the content of the heavy rare earth (HRE) element (Dy) was 1.428 at.%, or ~9% of the total rare earth (TRE) elements. These data demonstrate that a small amount of HRE can effectively enhance the magnetic properties. Moreover, the Br is influenced by the density of the magnets. As the Ga content increased, the density of the Nd–Fe–B magnet declined from 7.534 g/cm^3 to 7.480 g/cm^3, because the density of Ga (5.9 g/cm^3) is much lower than that of Nd–Fe–B (~7.5 g/cm^3). This decrease in density slightly reduces the saturation magnetization of the Nd–Fe–B magnets. In summary, the magnetic properties of the Nd–Fe–B sintered magnets were effectively enhanced through the addition of $Dy_{80}Ga_{20}$ powder.

Table 1. TRE (total rare-earth), HRE (heavy rare-earth) content, magnetic properties, and density of the starting magnet and those doped with $Dy_{80}Ga_{20}$.

$Dy_{80}Ga_{20}$/wt.%	TRE/at.%	HRE/at.%	Hcj/kOe	Br/kGs	(BH)max/MGOe	Squareness/%	Density/g·cm^{-3}
0	14.32	0	12.72	13.82	46.63	94	7.534
1	14.619	0.362	16.41	13.31	42.50	93	7.496
2	14.912	0.720	17.96	12.95	40.78	92	7.492
3	15.205	1.076	19.13	12.73	39.13	93	7.485
4	15.494	1.428	21.44	12.28	36.73	93	7.480

To investigate the element distribution in the doped Nd–Fe–B sintered magnets, the distributions of Dy, Nd, Fe, and Ga across the intergranular phase and matrix phase were studied by WDS line scan analysis. According to the results in Fig. 2, the Pr and Nd in the Nd–Fe–B magnets with added $Dy_{80}Ga_{20}$ alloy powder were mainly concentrated in the grain boundary layers, and the Fe was enriched in the matrix phase. In particular, the concentration of Dy on the matrix phase grain surface was much higher than in the center of the matrix phase. The above results indicate that, during the sintering process, the Dy diffuses into the matrix phase grains rather than the center of the $Nd_2Fe_{14}B$ grains. An $(Nd, Dy)_2Fe_{14}B$ shell surrounding the matrix phase is formed by the diffusion of Dy, and this shell provides much higher coercivity than the pure $Nd_2Fe_{14}B$.[9] The distribution of Ga in the doped magnet is dispersive, and thus Ga can be found in both the intergranular phase and the matrix grains. The Ga in the matrix phase partly enters the crystal lattice, which could decrease the saturation magnetization of the Nd–Fe–B magnets.[23]

To investigate the thermal stability of the Nd–Fe–B magnets, the irreversible magnetic flux loss (Hirr) of the doped magnets was studied after treatment at relatively high temperatures. The Hirr of the doped Nd–Fe–B magnets following 2 h exposure at 20 °C, 60 °C, 80 °C, 120 °C, and 150 °C is shown in Fig. 3. The cylindrical magnets have a diameter of ~10 mm and a length of ~8.7 mm. At temperatures below 60 °C, the Hirr of the samples with 0–4 wt.% added powder changed slightly. However, as the temperature increased, the disparity in Hirr became larger. The irreversible loss of the $Dy_{80}Ga_{20}$-free magnet after being exposed at 150 °C for 2 h was about 43%. However, for the magnet with 4 wt.% $Dy_{80}Ga_{20}$, the irreversible loss after exposure at the same temperature was less than 2.2%. This remarkable improvement in Hirr, which indicates enhanced thermal stability, is mainly attributable to the improved coercivity produced by the addition of $Dy_{80}Ga_{20}$ powder.[24]

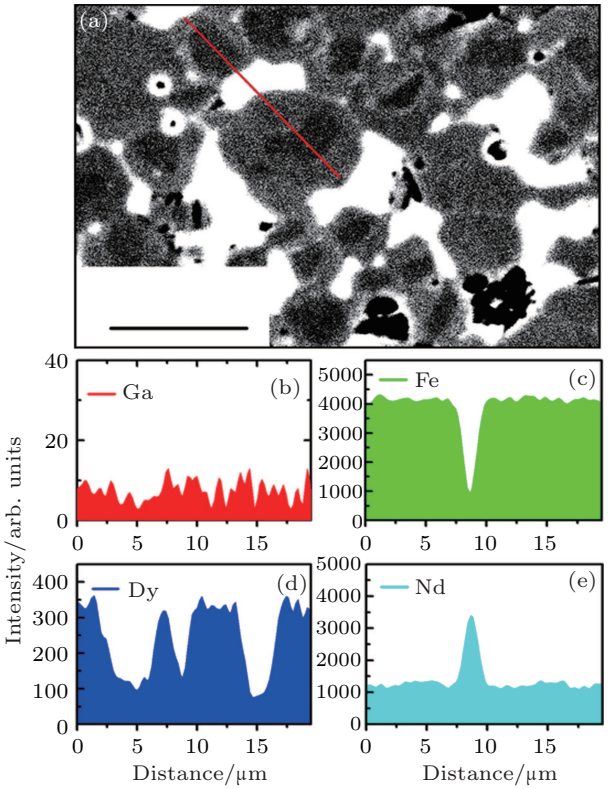


Fig. 2. (color online) The back-scattered image (a) and WDS results for the spatial distribution of Ga (b), Fe (c), Dy (d), and Nd (e) across the intergranular phase and matrix phase grains in $(Pr_{80}Nd_{20})_{31}Fe_{bal}B$ sintered magnets with 4 wt.% $Dy_{80}Ga_{20}$ addition.

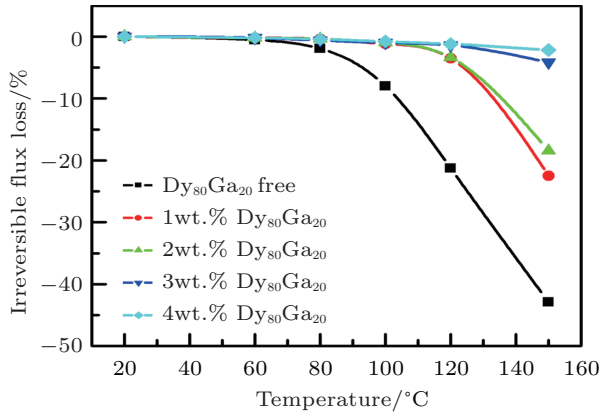


Fig. 3. (color online) Irreversible loss of magnetic flux in magnets with different amounts of $Dy_{80}Ga_{20}$ after being exposed at 20 °C, 60 °C, 80 °C, 120 °C, and 150 °C for 2 h.

To examine the thermal stability of the sintered Nd–Fe–B magnets, the temperature coefficients of remanence (α) and coercivity (β) were investigated. The magnetic properties of the sintered Nd–Fe–B magnets with added $Dy_{80}Ga_{20}$ were measured at room temperature (20 °C) and relatively high temperature (100 °C). Based on the data recorded at these temperatures, the temperature coefficients of remanence (α) and coercivity (β) are shown in Fig. 4. As the temperature was adjusted from 20–100 °C, the temperature coefficient of remanence (α) for the undoped magnet was measured at $-0.117\%\ °C^{-1}$, whereas that for the magnets with 4 wt.% $Dy_{80}Ga_{20}$ increased to $-0.106\%\ °C^{-1}$. Moreover, the temperature coefficient of coercivity (β) improved from $-0.74\%\ °C^{-1}$ to $-0.60\%\ °C^{-1}$ as the temperature increased. The partial substitution of Dy for Nd could compensate for the decrease in α because of the ferromagnetic coupling between Dy and Fe. In addition, the Ga atoms diffused into the matrix grains could decrease the negative exchange interaction of Fe–Fe, which is beneficial to a lower value of α.[25] The improvement in β was a result of the higher intrinsic anisotropy field of the highly magnetic $(Dy, Nd)_2Fe_{14}B$ shell.[26] With the improved temperature coefficient, it can be inferred that the thermal stability of the doped Nd–Fe–B magnets also improved.

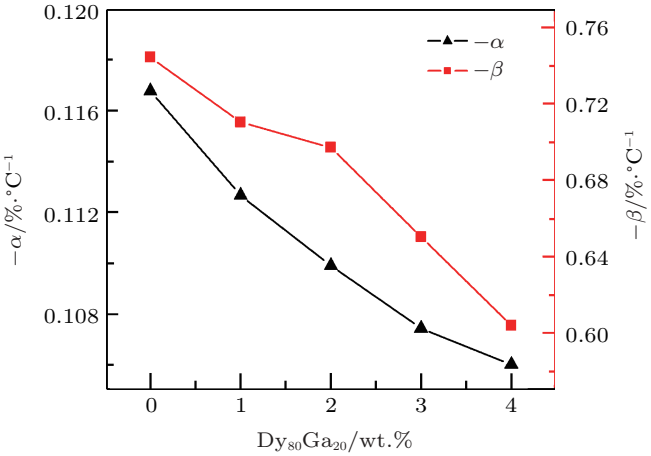


Fig. 4. (color online) Temperature coefficients (from 20–100 °C) of remanence (α) and coercivity (β) for the magnets.

The mass loss of the magnets following exposure to a corrosive environment (120 °C, 2 bar, and 100% relative humidity) for different periods was studied, and the results are shown in Fig. 5. For all the Nd–Fe–B sintered magnets, the mass loss increased after the magnets had been exposed to the corrosive environment for a longer period. After the first 24 h, the mass loss of the undoped magnets was about 1.84 mg/cm^2. When the exposure time increased to 96 h, the mass loss increased to 28.1 mg/cm^2, indicating that the corrosion rate increased. The magnets with added $Dy_{80}Ga_{20}$ exhibited lower mass loss than the undoped magnets. After the first 24 h, the mass loss of the magnets with 4 wt.% $Dy_{80}Ga_{20}$ was 0.52 mg/cm^2, some 1.32 mg/cm^2 lower than that of the undoped magnets. Furthermore, when the doped magnets were exposed to the corrosive environment for 96 h, the mass loss was only 2.68 mg/cm^2, much lower than the 28.1 mg/cm^2 of the undoped magnets. The relatively lower mass loss indicates improved corrosion resistance in the doped magnets. The corrosion of the Nd–Fe–B magnets mainly occurs in the intergranular phase, because of the low electrode potential of Pr and Nd in this region. The doped elements of Dy and Ga in the intergranular phase have higher electrode potential, and thus improve the corrosion resistance.

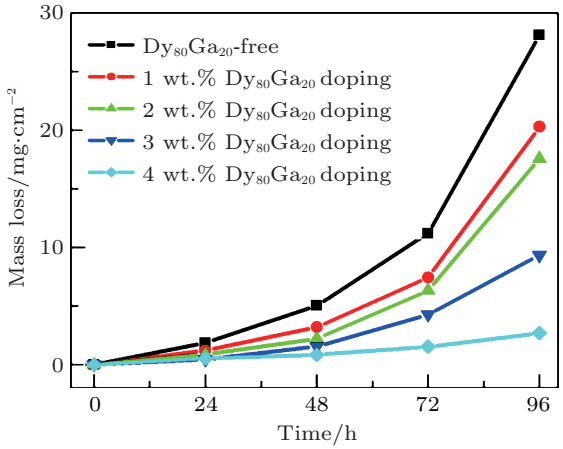


Fig. 5. (color online) Mass loss of magnets in a 120 °C, 2 bar, and 100% relative humidity atmosphere for 24, 48, 72, and 96 h.

4. Conclusions

This research studied the enhancement of magnetic properties, thermal stability, and corrosion resistance in Nd–Fe–B magnets with added $Dy_{80}Ga_{20}$ powder. The coercivity of the doped magnets was enhanced from 12.72 kOe to 21.44 kOe, with a corresponding decrease in remanence of just ∼11%. This was due to the refined and uniform matrix phase grains, continuous grain boundaries, and a hardened $(Nd, Dy)_2Fe_{14}B$ shell surrounding the matrix phase grains. After being exposed to high temperatures, the irreversible loss of magnetic flow in the doped magnets decreased sharply compared with that of the undoped magnets. For the Nd–Fe–B sintered magnets with 4 wt.% $Dy_{80}Ga_{20}$ powder, exposure at 150 °C for 2 h resulted in a Hirr of just ∼2.2%, approximately one-twentieth of that suffered by the undoped magnet. After doping with $Dy_{80}Ga_{20}$, the temperature coefficients of remanence (α) and coercivity (β) were also improved. The improvement in Hirr and the temperature coefficients indicates that the thermal stability of the magnets can be enhanced through the addition of $Dy_{80}Ga_{20}$ alloy powder. The reduced mass loss of the doped magnets shows that the corrosion resistance can also be improved. This is attributable to the enhanced electrode potential in the intergranular phase.

Acknowledgment

We are grateful to the Ningbo Institute of Materials Technology and Engineering of Chinese Academy of Sciences for the support in our experiment.

References

[1] Sagawa M, Fujimura S, Togawa N, Yamamoto H and Matsuura Y 1984 *J. Appl. Phys.* **55** 2083
[2] Gutfleisch O, Willard M A, Brück E, Chen C H, Sankar S G and Liu J P 2011 *Adv. Mater.* **23** 821
[3] Chen B C, Liu X M, Chen R J, Guo S, Yan C J, Lee D and Yan A R 2012 *J. Appl. Phys.* **111** 07A710
[4] Schultz L, El-Aziz A M, Barkleit G and Mummert K 1999 *Mater. Sci. Eng. A* **267** 307
[5] Ni J J, Ma T Y and Yan M 2012 *Mater. Lett.* **75** 1
[6] Liu J, Sepehri-Amin H, Ohkubo T, Hioki K, Hattori A, Schrefl T and Hono K 2013 *Acta Mater.* **61** 5387
[7] Hirosawa S, Matsuura Y, Yamamoto H, Fujimura S, Sagawa M and Yamauchi H 1986 *J. Appl. Phys.* **59** 873
[8] Boltich E, Oswald E, Huang M, Hirosawa S, Wallace W and Burzo E 1985 *J. Appl. Phys.* **57** 4106
[9] Yan G L, McGuiness P J, Farr J P G and Harris I R 2010 *J. Alloy. Compd.* **491** L20
[10] Komuro M, Satsu Y and Suzuki H 2010 *IEEE Trans. Magn.* **46** 3831
[11] Liu X L, Wang X J, Liang L P, Zhang P, Jin J Y, Zhang Y J, Ma T Y and Yan M 2014 *J. Magn. Magn. Mater.* **370** 76
[12] Cao X J, Chen L, Guo S, Li X B, Yi P P, Yan A R and Yan G L 2015 *J. Alloy. Compd.* **631** 315
[13] Wang X L, Zhao L N, Ding K H, Cui S L, Sun Y C and Li M S 2015 *Chin. Phys. B* **24** 037506
[14] Yan G L and Fang Z H 2015 *Chin. Phys. B* **24** 107503
[15] Zhang X F, Guo S, Yan C J, Cai L W, Chen R J, Lee D and Yan A R 2014 *J. Appl. Phys.* **115** 17A757
[16] Pandian, Chandrasekaran V, Markandeyulu G, Iyer K and Rao K R 2002 *J. Appl. Phys.* **92** 6082
[17] Kianvash and Harris I 1991 *J. Appl. Phys.* **70** 6453
[18] Grieb, Pithan C, Henig E T and Petzow G 1991 *J. Appl. Phys.* **70** 6354
[19] Strzeszewski, Hadjipanayis G and Kim A 1988 *J. Appl. Phys.* **64** 5568
[20] Pollard, Grundy P, Parker S and Lord D 1988 *IEEE Trans. Magn.* **24** 1626
[21] Ni J J, Ma T Y, Wu Y R and Yan M 2010 *J. Magn. Magn. Mater.* **322** 3710
[22] Wan F M, Zhang Y F, Han J Z, Liu S Q, Liu T, Zhou L, Fu J B, Zhou D, Zhang X D, Yang J B, Yang Y C, Chen J and Deng Z W 2014 *J. Appl. Phys.* **115** 203910
[23] Sugimoto S, Gutfleisch O and Harris I R 1997 *J. Alloy. Compd.* **260** 284
[24] Ma B M, Liu W L, Liang Y L, Scott D W and Bounds C O 1994 *J. Appl. Phys.* **75** 6628
[25] Gauder D R, Froning M H, White R J and Ray A E 1988 *J. Appl. Phys.* **63** 3522
[26] Cui X G, Cui C Y, Cheng X N and Xu X J 2014 *Intermetallics* **55** 118